HIROSAKI UNIVERSITY

Radiation Environment and Medicine 2023 Vol.12, No.2 81–90

REM
Radiat Environ Med

Review

Biophysical Simulations for Estimating Biological Effects after Exposure to Ionizing Radiation: Current State and Future Prospects

Yusuke Matsuya[1, 2]* and Ryo Saga[3]

[1] *Faculty of Health Sciences, Hokkaido University, Kita-12, Nishi-5, Kita-ku, Sapporo 060-0812, Japan*
[2] *Nuclear Science and Engineering Center, Japan Atomic Energy Agency, Shirakata 2-4, Tokai 319-1195, Japan*
[3] *Department of Radiation Science, Graduate School of Health Sciences, Hirosaki University, 66-1 Hon-cho, Hirosaki, Aomori, 036-8564, JAPAN*

Received 5 April, 2023; revised 6 June, 2023; accepted 14 June, 2023

Monte Carlo radiation transport simulations and biophysical models are powerful tools to evaluate the biological effects after exposure to ionizing radiation in radiation protection and radiation therapy. During human body exposure to radiation, DNA lesions as an early biological response are induced by energy deposition, leading to cell death with a certain probability. Thus, conducting translational studies focusing on radiation physics, cellular biology, and oncology is warranted. Herein, two simulation tools for predicting biological effects are introduced, that is, Particle and Heavy-Ion Transport code System (PHITS) and integrated microdosimetric-kinetic model (IMKM). To date, the PHITS code, which implements track-structure calculation at a DNA scale, allows estimation of the DNA damage yields through electrons and protons in various forms, such as single-strand break (SSB), double-strand break (DSB), and complex DSB (that is DSB coupled with additional strand breaks within 10-bp separation). Meanwhile, the IMKM which was developed to consider microdosimetry, the DSB damage responses and heterogeneous cell population can successfully reproduce experimental cell surviving fraction for various irradiation conditions, which can realize the translational study between *in vitro* cell survival and clinical tumor control probability in cancer treatment. These models would allow a precise understanding of cellular responses after exposure to ionizing radiation. Throughout this review, we discuss the latest status and future prospects of these simulation tools.

Key words: track-structure simulation, biophysical model, DNA damage, cell surviving fraction, tumor control probability

1. Introduction

Energy deposition as a biological sequela of ionizing radiation can induce mutations, cell death, and carcinogenesis[1]. While cell-killing effects against cancer can be used as a positive phenomenon in radiation therapy, radiation-induced biological effects should be minimal as far as possible. Cell death is mainly induced by DNA lesions, particularly double-strand breaks (DSBs) with a certain probability[2-4]. Energy deposited by atomic interactions of radiation (physical processes) and subsequent reaction of free radicals to DNA (chemical processes) are the major pathways of inducing DNA damage, referred to as direct and indirect effects[5]. Therefore, when evaluating the biological effects after

*Yusuke Matsuya: Faculty of Health Sciences, Hokkaido University, Kita-12, Nishi-5, Kita-ku, Sapporo 060-0812, Japan
E-mail: matsuya.yusuke@hs.hokudai.ac.jp (Yusuke Matsuya)
https://doi.org/10.51083/radiatenvironmed.12.2_81

radiation exposure, the mechanisms of early DNA damage induction based on physics play a key role. A simulation approach based on physical processes for estimating radiation-induced biological effects is a challenging research topic but is effective for clarifying cellular mechanisms, which has gained popularity worldwide.

When evaluating early biological responses, the Monte Carlo track-structure simulation codes which enable simulating each atomic interaction (such as ionization and electronic excitation) are useful. There are various kinds of track-structure simulation codes such as PARTRAC[6], Kyushu University Radiobiology Unit Code (KURBUC)[7, 8], Geant4-DNA[9-11], RITRACK[12, 13], NASIC[14], TRACEL[15], MCNP6[16], WLTrack[17], and Particle and Heavy Ion Transport code System (PHITS)[18]. Some existing codes such as Geant4-DNA and PHITS are available free of charge, whereas most of them are private code not available without the developer's permission. Using a spatial pattern of deposited energy or atomic interaction density in a small target composed of liquid water, the yields of early DNA damage (i.e., single-strand break [SSB], DSB, and complex DSB) after ionizing radiation exposure have been calculated[19-22]. The DNA damage simulation plays an important role in elucidating the induction mechanisms of initial DNA damage yields after exposure[23, 24]. Particularly, the complex DSB (that is DSB coupled with additional strand breaks within 10-bp separation), which is recognized as a refractory lesion but is difficult to be experimentally detected, can be quantitatively estimated through the simulation approach. However, the computational time for calculating DNA damage yields is generally prolonged because chemical simulation for free radicals[25, 26] is a time-consuming method. Therefore, development of a DNA damage estimation model with a short computational time is warranted.

Meanwhile, for biological effects such as cell death, a simple mathematical model named the linear-quadratic (LQ) model is traditionally used[27-29]. The LQ model enables interpolation of experimentally measured dose-response curve of surviving fraction; however, the model must be applied to experimental results measured for each irradiation condition. Meanwhile, a few mechanistic models have been proposed by researchers to predict surviving fraction for various radiation qualities representing linear energy transfer (LET), such as microdosimetric-kinetic (MKM)[30, 31] and local effect model (LEM)[32]. Once MKM is applied to the *in vitro* cell survival curve after photon irradiation, MKM allows estimation of the curves for various LET irradiations[33] and is advantageous in applying estimates of cell killing after particle therapy such as protons, carbon ions, and multi-ions[34-36]. In recent decades, detailed mechanistic models based on physical, chemical, and biological processes have been proposed, that is, modified MKM[37], BIophysical ANalysis of Cell death and chromosome Aberrations (BIANCA)[38], NANodosimetry and OXydative (NanOX)[39], stochastic MKM (SMKM)[40, 41], and integrated MKM (IMKM)[42]. As such, biophysical models have been used for investigating cellular mechanisms related to radiosensitivity (i.e., cell killing).

Here, we introduce two simulation tools for predicting biological effects, namely, PHITS, and IMKM. The PHITS code is a general-purpose Monte Carlo code which have been used for various applications such as radiation shielding, medical physics, and geosciences[18]. To date, the track-structure modes in the PHITS code, so-called *PHITS-ETS*[43] and *PHITS-KURBUC*[44], have been developed, and an analytical code for predicting DNA damage yields based on the modes has been included in the PHITS package[43]. Meanwhile, to estimate the radiosensitivities for various experimental conditions, IMKM has a unique biophysical model considering the physical, chemical, and biological factors[33, 45-48]. IMKM has successfully reproduced *in vitro* cell surviving fraction and clinical tumor control probability (TCP)[48]. In radiation protection and radiation therapy, a precise understanding of cellular radiation responses after exposure to ionizing radiation can be achieved through the combination of these estimation tools. In this review, we discuss the latest status and future plans of these simulation tools.

2. Particle and Heavy Ion Transport Code System (PHITS)

The PHITS code[18] is one of radiation transport simulation codes which have been developed worldwide. The code can handle most of the particle types with energies up to 1 TeV/n using several nuclear reaction models and data libraries. There are two types of radiation transport modes: one is condensed-history method for macroscopic calculation at the cm scale and track-structure simulation considering each atomic interaction at the DNA (nm) scale[49]. As for the former mode, the PHITS code uses the ATIMA mode (http://web-docs.gsi.de/~weick/atima) and electron gamma shower (EGS) mode[50] available for arbitrary materials. Meanwhile, the latter track-structure mode can generate realistic tracks of electrons, positrons, protons, and carbon ions in liquid water[43, 44]. The track-structure mode has been used for investigating biomolecular dissociation processes as a physical study[51]. Using the spatial patterns of atomic interactions (ionizations and electronic excitations) calculating the track-structure modes, the SSB, DSB, and complex DSB yields can be estimated[49]. The DNA damage yield stimulation is illustrated in Figure 1.

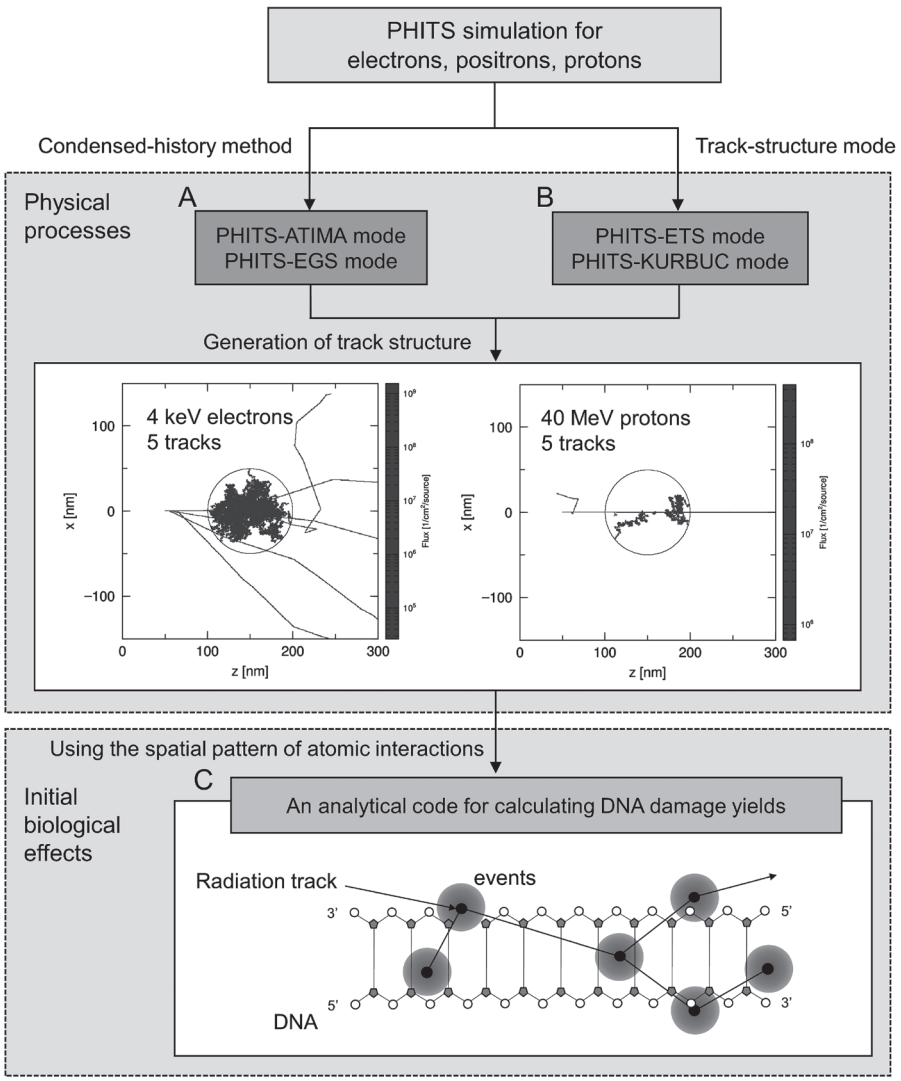

Fig. 1. Flow of DNA damage yield estimation using the Particle and Heavy-Ion Transport code System (PHITS) code. When using the track-structure modes (*PHITS-ETS, PHITS-KURBUC*)[43, 44], the coordinates of atomic interactions are firstly calculated. Second, the number of events (ionizations and excitations), linkage (which is a pair within 10-bp separation), and DNA damage (strand break and double-strand break [DSB]) yields for each radiation track is estimated. The current DNA damage simulation model can be available for electrons, positrons, and protons[43, 65].

2.1. Track-structure mode for physical processes

In 2018, to extend the transport of electrons and positrons down to 10^{-3} eV[18], a track-structure mode for electrons and positrons in PHITS was developed, which is called *PHITS-ETS* or *etsmode*[43]. Other codes such as Geant4-DNA can simulate kinetics of electrons only for energies down to 7.4 eV[52]. Comparing *PHITS-ETS* with other codes, the electron transport using a lower energy than 7.4 eV is an advantage. To simulate each atomic interaction in liquid water, the *PHITS-ETS* mode considers the cross-sections of elastic scattering, five ionizations, six excitations, dissociative electron attachment, vibrational excitations, photon excitations, and rotational excitations, which are used in the dynamic Monte Carlo Code (DMCC)[53-56]. These cross-sections for electrons are dedicated for liquid water. Meanwhile, the path length of electron in material other than water can be scaled based on electron densities of material, and the scaling model has been benchmarked compared to the track length using the EGS mode[49]. The *PHITS-ETS* mode has been available for PHITS version after 3.02. Additionally, in 2022, the track-structure mode for silicon (so-called *PHITS-ETS for Si*) has been recently developed, which is useful for investigating radiation detectors such as semiconductor devices[57].

In 2020, in collaboration with Nikjoo, and Liamsuwan, developers of the track-structure code named as KURBUC, the track-structure mode for protons and carbon ions in liquid water has been developed[44]. The mode uses the KURBUC algorithms for the ions and

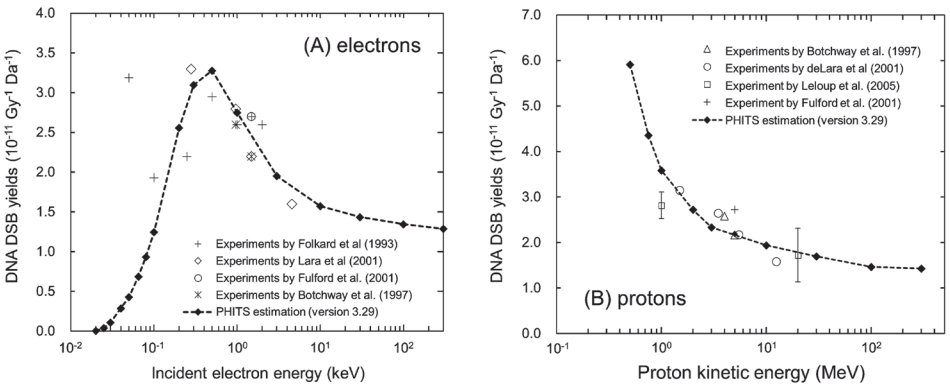

Fig. 2. DSB yields calculated using the PHITS code. (A) DSBs induced after electron exposure and (B) DSBs induced after proton exposure[44, 65]. To calculate the yields, activation of the *PHITS-ETS* mode occurs when electrons are transported until they fully stop within liquid water. Meanwhile, in calculating the yields for protons, 1% of the proton energy is being deposited in this region when *PHITS-KURBUC* is activated.

PHITS-ETS for electron transport, which is named as *PHITS-KURBUC*. The *PHITS-KURBUC* mode considers the cross-sections of ionizations, excitations, and charge exchange, which was implemented in KURBUC code[58-60]. The available energy ranges of protons and carbon ions are from 1 keV to 300 MeV and from 1 keV/n to 10 MeV/n, respectively. The *PHITS-KURBUC* mode is implemented in PHITS version after 3.20. In 2021, the Ion Track-Structure model for Arbitrary Radiation and Targets referred to as *ITSART* has been further developed[61], which is implemented in *PHITS* version after 3.25. The current *ITSART* mode considers the ionization cross-sections and is now under development to demonstrate elastic scattering, excitation, and charge exchange.

Thus far, these modes have been benchmarked by comparing the range, stopping power, and microdosimetry calculated by the track-structure modes to other simulation and recommended data (such as the ICRU report)[43, 44, 49]. One of the advantages of the track-structure modes in PHITS is not only considering the discrete levels of ionizations, excitations, and molecular excitations but also enabling simulating the spatial distributions at a DNA scale. The discrete levels can be used when evaluating generation of free radicals (physicochemical processes)[62]. Meanwhile, ionization and excitation patterns can be useful for investigating mechanisms of DNA damage induction[6, 63]. In addition, the chemical simulation also plays a key role in investigating mechanisms on DNA damage induction[5]. The chemical code dedicated for PHITS is now under development and will be included in the PHITS package in the near future.

2.2. DNA damage simulation based on atomic interactions

In the PHITS package in the PHITS version after 3.10, an analytical code for estimating the yields of DNA lesions is included[43]. The DNA damage estimation model in PHITS is simple, which uses the spatial patterns of ionizations and excitations (so-called events). In the model, the frequency of events per energy deposition and that of linkages (composed of two events within the 10-bp separation) per energy are assumed to be proportional to the yields of strand break (SB) and DSB, respectively[43]. Furthermore, the DSB coupled with an SB and that with two SBs within 10-bp separation (which are defined as DSB+ and DSB++) can be estimated by scoring the number of events within a 10-bp radius sphere[64]. The DSB+ and DSB++ are called complex DSB in this review. The criteria for predicting the complex DSBs are 2–14 for a simple DSB, 14–26 for DSB+, and 26–38 for DSB++. These DNA damage yields have been traditionally estimated by energy deposited within a small target or ion cluster size[19, 21]. The model of the PHITS code can efficiently sample these frequencies of events and linkages within a region where the track-structure mode is activated, leading to an efficient estimation of the SSB, DSB, and complex DSB yields within a short calculation time.

The accuracy of the DNA damage estimation model has been benchmarked by comparing the estimation by the model with the corresponding experimental data. Figure 2 shows the energy dependence of DSB yields for (A) electrons and (B) protons, in which the yields for electrons and protons were estimated using the *PHITS-ETS* and the *PHITS-KURBUC* modes, respectively[43, 65]. As shown in Figure 2, the yields by the PHITS code were compared to the experimental results, showing good agreements between the simulation and experimental data. The accuracy of the SSB yield (as well as the relative biological effectiveness [RBE]) estimated by PHITS was evaluated and compared to the other simulations (such as PARTRAC and Geant4-DNA) and experimental data[66-71], as reported previously[49, 65]. The DSB+ and DSB++ cannot be directly observed via

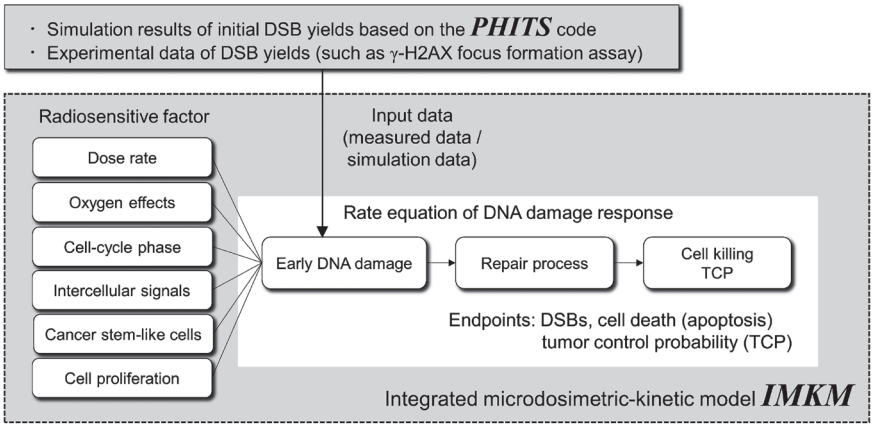

Fig. 3. Overview of the integrated microdosimetric-kinetic model (IMKM). Setting the radiosensitive factor by researchers, the IMKM allows estimation of cell killing (surviving fraction) and TCP[42, 48]. To date, the model considers microdosimetry, oxygen effects, DNA repair during irradiation, cell-cycle phase, intercellular signaling, existence of cancer stem-like cells, and cell proliferation. Using data from calculated or measured DNA damage yields, the IMKM can be used as a mechanistic study for cellular responses after ionizing radiation exposure[45, 83].

an experimental approach. To solve this problem, the experimental yields of DSBs coupled with base lesions (so-called clustered DSB) induced after 70 kVp X-rays, which was detected by atomic force microscopy[72], were used to validate the model in PHITS. As a result, it was shown that scoring of the number of events within a 10-bp radius sphere is simple but sufficient for reproducing the experimental yields of clustered DSBs[64]. To date, the model was further validated by comparing it with the photon-induced γ-H2AX focus size representing DSB complexity[73]. The γ-H2AX focus formation assay is well known as an experimental method that can detect the DSB site within cultured cells after irradiation[74-77].

The current DNA damage estimation model enables the efficient estimation of DNA damage yields only for low-LET radiations (i.e., < 30 keV/μm)[65]. This is because in this model, the implicit consideration of chemical reactions has some drawbacks. Therefore, the influence of LET is not explicitly accounted for. Other simulations using the KURBUC and PARTRAC codes consider the indirect effects induced after chemical processes (i.e., the G value of hydroxyl radical [radical])[78, 79]. To employ the DNA damage model to high-LET irradiation, developing a chemical simulation code is necessary to further develop a mechanistic study and a simple chemical model for expressing LET dependence on indirect DNA damage yields for efficient estimation in the near future.

3. Integrated Microdosimetric-Kinetic Model (IMKM)

To investigate the dose-rate effects after protracted exposure, the IMKM was developed to assess the DNA repair during irradiation (DNA targeted effects) and non-targeted effects (NTEs) after low-dose acute irradiation[42, 80-82]. In the IMKM, a cell nucleus is divided into hundreds of micron-order territories (so-called domains) which are in general defined as 1–2-μm diameter spheres to evaluate the heterogeneous energy deposition in the cell. To demonstrate the DNA damage responses during and after irradiation by using the rate equations, two lesions, that is, potentially lethal lesion (PLL) and lethal lesion (LL), are assumed[46]. The PLL and LL mean reparable lesion and non-reparable one, respectively. To date, IMKM has been developed to consider microdosimetry[33], oxygen effects[45], DNA repair during irradiation[46, 80-82], cell-cycle phase[46], NTEs (i.e., bystander effects and protective effects induced by intercellular communication between irradiated cells and non-irradiated cells)[42, 83], existence of cancer stem-like cells[47], and cell proliferation[48]. As shown in Figure 3, using the physical, and biological information previously, for example, radiation quality, oxygen pressure, and content of cancer stem-like cells, IMKM can predict surviving fraction of mammalian cells and TCP of cancer as a function of absorbed dose.

3.1. Prediction of cell survival considering various factors

Considering the development based on the MKM, the IMKM allows for the estimation of LET dependence on biological effects (i.e., RBE), and the dose-rate effects for various LET radiations[33]. To consider LET dependence, the dose-mean lineal energy (y_D value)[84] with saturation-correction at a higher LET than approximately 100 keV/μm is considered in the model. Using the tally (named as *t-sed*) in PHITS, the y_D value can be easily calculated[85]. For example, the IMKM was used to evaluate the surviving fraction of melanoma after boron neutron capture therapy (BNCT), in which ^{10}B is administered to cancer cells and is rendered as one of the most effective approaches for malignant tumor treatment using high-

LET α particles and Li ions generated by $^{10}B(n, \alpha)^{7}Li$ reaction[86, 87]. From the model analysis, compared to ^{60}Co-rays irradiation with low LET, the model estimation exhibited a reduced impact on cell recovery during high-LET irradiation[33].

Through the repair dynamics of PLL, the IMKM can be applied to study the biological effects after protracted exposure. The repair of PLLs during irradiation considered in the IMKM was found to correspond to DSB repair from the γ-H2AX focus formation assay[88]. At a high-dose range, the DSB repair during irradiation can illustrate the characteristics of log of surviving fraction in a rectilinear form[80, 81]. Traditionally, to express the rectilinear form, several biophysical models, such as the universal survival curve (USC)[89] and LQ-Linear (LQ-L) model[90], have been proposed; however, the IMKM can mechanistically illustrate the rectilinear form using the correlation factor, that is, the reduction of coefficient to dose square β (Gy^{-1}), which is called the Lea-Catchesides time factor[91]. Furthermore, cell-cycle distributions (where are intrinsically related to radiosensitivity) can be modified depending on dose rate during the protracted exposure[46, 81]. The cell-cycle change of Chinese Hamster cell (CHO-K1) during irradiation was considered as the changes of DNA amount per cell and the S-phase-dependent repair efficiency[46]. Using the experimental cell-cycle change, the model simulation suggested that the change in cell-cycle phase during protracted irradiation with 250-kVp X-rays modulates the dose-response curve and is possibly responsible for some inverse dose-rate effects in mammalian cells[46].

The impact of radiosensitivity can be enhanced by intercellular signaling from radiation-hit cells to non-hit cells. The time course of intercellular signals (such as calcium[92] and nitric oxide[93]) has been modeled in the IMKM[42]. In the model, a target of intercellular signal release (which is defined as cell-killing signals in the model) is micron-order site (domain)[94, 95] linked to mitochondria[96]. Particularly, to release the signals, the number of hits follows a linear-quadratic function of dose imparted in a domain[42]. Assuming that the yield of LL in non-hit cells is proportional to the fractions of hit cells and non-hit cells, the IMKM enables estimation of cell killing of both normal fibroblasts and various cancer cells induced by intercellular signaling (NTEs) after acute exposure. To date, using the model, IMKM has successfully reproduced the experimental low-dose hyper-radiosensitivity and bystander effects[42]. Furthermore, the model is useful when investigating the radiosensitizing mechanisms of cancer cells through the hyaluronan synthesis inhibitor 4-methylumbelliferone (4-MU)[97]. Among the several outcomes of this model, a successful theoretical analysis of the impacts of modulated radiation fields on radiosensitivity and cell recovery during dose delivery was conducted[83]. In 2020, the DSB yields depending on the oxygen pressure was considered in the IMKM, which enables prediction of the oxygen enhancement ratio (oxygen effects)[45]. By integrating intercellular signals and oxygen effects, the latest IMKM facilitates a more precise understanding of intercellular signaling and oxygen effects following exposure to intensity-modulated radiation fields for cancer therapy[98, 99].

3.2. Application of the IMKM to clinical studies

During *in vitro* radiosensitivity analysis, the use of IMKM, assuming that cultured cells are composed of a homogeneous cell population, is sufficient. However, the actual tumor tissue affected by radiotherapy is composed of heterogenous cell populations, that is, non-radioresistant cells (progeny cells) and radioresistant cells (cancer stem-like cells)[100]. Both radiosensitivity and curative effects are largely dependent on the biological factors based on the 4 "R's" concept, namely, repair, redistribution, repopulation, and reoxygenation[101]. Additionally, the fifth biological factor, "radiosensitivity" (heterogeneity of radiosensitivity) has been highlighted recently[102, 103]. Considering these, since 2019, we started to develop IMKM to explicitly consider the existence of cancer stem-like cells[47].

The first model analysis for cancer stem-like cells was performed by applying the IMKM to the experimental dose-response of surviving fraction after X-ray irradiation using three types of prostate cancer cells (DU145, PC3, and LNCaP)[47]. In the fitting approach results, we found that the model which considered the existence of cancer stem-like cells illustrated the sigmoid nature regarding the relationship between dose and log of surviving fraction and showed good agreement with the experimental *in vitro* survival[47]. Next, the cancer stem-like cells within human oral squamous carcinoma cell lines (SAS and HSC2) were investigated through cell experimentation and model estimation[104]. Because of the difficulty to perform cell experiments on heterogeneous cell populations using the standard cell line, we used the radioresistant cell line named SAS-R and HSC2-R, which has been established after daily exposure to 2 Gy of X-rays for more than 1 year[105]. From the flow cytometric analysis using a ALDH maker for detecting cancer stem-like cells, SAS-R and HSC2-R cell lines were found to contain more cancer stem-like cells than SAS and HSC2. From the hybrid study, it was found that enhanced cell recovery of cancer stem-like cells is important when predicting cell-killing effects in radiotherapy which requires a long dose-delivery time[104].

Based on the model development, focusing on the stereotactic body radiotherapy (SBRT) for non-small cell lung cancer (NSCLC), we recently developed the all-in-one model (IMKM), which allows estimation of

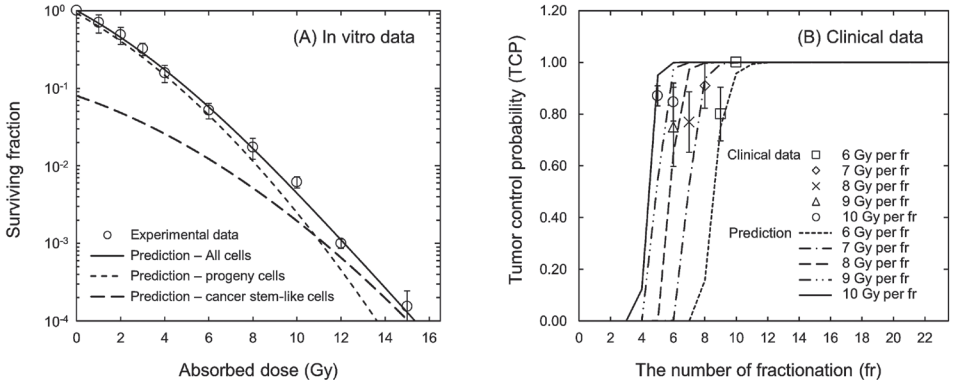

Fig. 4. Prediction of curative effects by the IMKM.
(A) *In vitro* surviving fraction and (B) TCP for various fractionation regimens. When estimating both *in vitro* surviving fraction and clinical TCP, the cancer stem-like cells (7.983%) were considered. Using the same contents and model parameters, the IMKM has successfully reproduced the *in vitro* cell survival and clinical TCP after the stereotactic body radiotherapy for non-small cell lung cancer[48].

TCP of cancer patients as well as surviving fraction, and attempted to investigate the impact of cancer stem-like cells on curative effects (TCP)[48]. As a result, as shown in Figure 4, considering cancer stem-like cells, we have successfully reproduced both *in vitro* survival of A549 (NSCLC cell line) after acute irradiation and the 3-year (as well as 5-year and 8-year) TCP with various fractionation plans (6–10 Gy/fr)[106, 107]. The IMKM developed thus far would contribute to high-precision estimation of the curative effects of SBRT on NSCLC. Meanwhile, the time course of radiosensitivity after high-dose exposure and the mechanisms on how to acquire radioresistance after high-dose irradiation remain unclear. Considering these, accumulation of *in vitro* and *in vivo* scientific data and further model development to reproduce curative effects for any treatment cases (such as tumor types and irradiation conditions) are essential in the future.

4. Summary and future prospects

In this review, we introduce two simulation tools for predicting biological effects, namely PHITS, and IMKM. To date, the PHITS code has successfully reproduced the yields of various DNA damage, such as SSB, DSB, and complex DSB (DSB+ and DSB++) induced by electrons and protons. Meanwhile, the IMKM considers various radiosensitive parameters, such as microdosimetry, DSB repair kinetics, intercellular signaling, oxygen effects, and existence of cancer stem-like cells. The IMKM has also reproduced experimental surviving fraction for various irradiation conditions (radiation qualities, dose rate, oxygen pressure, and cell type), enabling the translational study between *in vitro* survival and clinical TCP for cancer therapy.

These simulation tools would contribute to a precise understanding of biological effects (such as DNA damage response and cell killing) to ionizing radiation. Meanwhile, the current DNA damage estimation model is available only for electron and protons. To expand the applicability of the DNA damage simulation, the development of a chemical code and the model is currently underway. In addition, a comprehensive mechanistic model for estimating various biological endpoints (micronuclei, chromosome aberration, inflammation, and carcinogenesis) for normal tissue does not exist. Recently, an estimation model for tissue reaction is required[108]. The aim of the simulation tools (model) is to become a spring board for improving the theoretical/computational models of the biological effects for radiobiology. Accumulation of experimental data for further model development and for predicting cellular responses after ionizing radiation exposure in the future is warranted.

Conflict of interests

The authors declare that they have no conflict of interest.

References

1. Joiner MC, van der Kogel AJ, Steel GG. Introduction: the significance of radiology and radiotherapy for cancer treatment. In: Joiner M, van der Kogel AJ, editors. Basic Clinical Radiobiology. London: Edward Arnold; 2009. p. 1–10.
2. Olive PL. The role of DNA single- and double-strand breaks in cell killing by ionizing radiation. Radiat Res. 1998;150:Suppl:S42–S51.
3. Carante MP, Altier S, Bortolussi S, Postuma I, Protti N, Ballarini F. Modeling radiation-induced cell death: role of different levels of DNA damage clustering. Radiat Environ Biophys. 2015;54:305–16.
4. Ballarini F, Altieri S, Bortolussi S, Carante M, Giroletti E, Protti N. The BIANCA model/code of radiation-induced cell death: application to human cells exposed to different radiation types. Radiat Environ Biophys. 2014;53:525–33.
5. Hall EJ, Giaccia AJ. Physics and Chemistry of Radiation Absorption. In: Radiobiology for the Radiologist. 7th ed.

Philadelphia Lippincott Williams & Wilkins; 2006. p. 3–11.

6. Friedland W, Dingfelder M, Kundrát P, Jacob P. Track structures, DNA targets and radiation effects in the biophysical Monte Carlo simulation code PARTRAC. Mutat Res. 2011;711(1–2):28–40.
7. Uehara S. The development of a Monte Carlo code simulating electron–photon showers and its evaluation by various transport benchmarks. Nucl Instrum Methods B. 1986;14:559–70.
8. Nikjoo H, Uehara S, Emfietzoglou D. Interaction of Radiation with Matter. Boca Raton, FL: CRC Press; 2012.
9. Incerti S, Baldacchino G, Bernal M, Capra R, Champion C, Francis Z, *et al*. The Geant4-DNA project. Int J Model Sim Sci Comput. 2010;1(2):157–78.
10. Incerti S, Ivanchenko A, Karamitros M, Mantero A, Moretto P, Tran HN, *et al*. Comparison of Geant4 very low energy cross section models with experimental data in water. Med Phys. 2010;37:4692–708.
11. Bernal MA, Bordage MC, Brown JMC, Davídková M, Delage E, El Bitar Z, *et al*. Track structure modeling in liquid water: a review of the Geant4-DNA very low energy extension of the Geant4 Monte Carlo simulation toolkit. Phys Med. 2015;31:861–74.
12. Plante I, Cucinotta FA. Ionization and excitation cross sections for the interaction of HZE particles in liquid water and application to Monte-Carlo simulation of radiation tracks. New J Phys. 2008;10:1–15.
13. Plante I, Cucinotta FA. Monte-Carlo simulation of ionizing radiation tracks. In: Mode CJ, editor. Application of Monte Carlo Methods in Biology, Medicine and Other Fields of Science. Rijeka, Croatia: InTech; 2011. p. 315–56.
14. Li J, Li C, Qiu R, Yan C, Xie W, Wu Z, *et al*. DNA strand breaks induced by electrons simulated with Nanodosimetry Monte Carlo Simulation Code: NASIC. Radiat Prot Dosim. 2015;166(1–4):38–43.
15. Tomita H, Kai M, Kusuma T, Ito A. Monte Carlo simulation of physicochemical processes of liquid water radiolysis. Radiat Environ Biophys. 1997;36:16–22.
16. Hughes G. Recent developments in low-energy electron/photon transport for MCNP6. Prog Nucl Sci Technol. 2014;4:454–58.
17. Date H, Sutherland KL, Hasegawa H, Shimozuma M. Ionization and excitation collision processes of electrons in liquid water. Nuc Instr Meth B. 2007;265(2):515–20.
18. Sato T, Iwamoto Y, Hashimoto S, Ogawa T, Furuta T, Abe S, *et al*. Features of Particle and Heavy Ion Transport code System (PHITS) version 3.02. J Nucl Sci Technol. 2018;55(5–6):684–90.
19. Goodhead DT, Leenhouts HP, Paretzke HG, Terrissol M, Nikjoo H, Blaauboer R. Track structure approaches to the interpretation of radiation effects on DNA. Radiat Prot Dosim. 1994;52(1–4):217–23.
20. Nikjoo H, O'Neill P, Goodhead DT, Terrissol M. Computational modelling of low-energy electron-induced DNA damage by early physical and chemical events. Int J Radiat Biol. 1997;71(5):467–83.
21. Grosswendt B, Pszona S, Bantsar A. New descriptors of radiation quality based on nanodosimetry, A first approach. Radiat Prot Dosim. 2007;126(1–4):432–44.
22. Yoshii Y, Sasaki K, Matsuya Y, Date H. Cluster analysis for the probability of DSB site induced by electron tracks. Nucl Instr Methods Phys Res B. 2015;350:55–9.
23. Petrolli L, Tommasino F, Scifoni E, Lattanzi G. Can we assess early DNA damage at the molecular scale by radiation track structure simulations? A tetranucleosome scenario in Geant4-DNA. Front. Phys. 2020;8:576284.
24. Kyriakou I, Tremi I, Georgakilas AG, Emfietzoglou D. Microdosimetric investigation of the radiation quality of low-medium energy electrons using Geant4-DNA. Appl Radiat Isot. 2021;172:109654.
25. Kreipl MS, Friedland W, Paretzke HG. Time- and space-resolved Monte Carlo study of water radiolysis for photon, electron and ion irradiation. Radiat Environ Biophys. 2009;48:11–20.
26. Shin W-G, Ramos-Mendez J, Tran NH, Okada S, Perrot Y, Villagrasa C, *et al*. Geant4-DNA simulation of the pre-chemical stage of water radiolysis and its impact on initial radiochemical yields. Phys Med. 2021;88:86–90.
27. Joiner MC. Quantifying cell kill and cell survival. In: Joiner MC, vander Kogel A, editors. Basic Clinical Radiobiology. 4th ed. London: Edward Arnold; 2009. p. 41–55.
28. Bentzen S, Joiner M, van der Kogel A. The linear-quadratic approach in clinical practice. In: Joiner MC, vander Kogel A, editors. Basic Clinical Radiobiology. 4th ed. London: Edward Arnold; 2009. p. 120–34.
29. McMahon SJ. The linear quadratic model: usage, interpretation and challenges. Phys Med Biol. 2019;64:01TR01.
30. Hawkins RB. A statistical theory of cell killing by radiation of varying linear energy transfer. Radiat Res. 1994;140:366–74.
31. Hawkins RB. A microdosimetric-kinetic model of cell death from exposure to ionizing radiation of any LET, with experimental and clinical applications. Int J Radiat Boil. 1996;69:739–55.
32. Grün R, Friedrich T, Elsässer T, Krämer M, Zink K, Karger CP, *et al*. Impact of enhancements in the local effect model (LEM) on the predicted RBE-weighted target dose distribution in carbon ion therapy. Phys Med Biol. 2012;57:7261–74.
33. Matsuya Y, Fukunaga H, Omura M, Date H. A model for estimating dose-rate effects on cell-killing of human melanoma after boron neutron capture therapy. Cells 2020;9:1117.
34. Inaniwa T, Suzuki M, Furukawa T, Kase Y, Kanematsu N, Shirai T, *et al*. Effects of dose-delivery time structure on biological effectiveness for therapeutic carbon-ion beams evaluated with microdosimetric kinetic model. Radiat Res. 2013;180:44–59.
35. Takada, K, Sato T, Kumada H, Koketsu J, Takai H, Sakurai H, *et al*. Validation of the physical and RBE-weighted dose estimator based on PHITS coupled with a microdosimetric kinetic model for proton therapy. J Radiat Res. 2018;59(1):91–9.
36. Inaniwa T, Kanematsu N. Adaptation of stochastic microdosimetric kinetic model for charged-particle therapy treatment planning. Phys Med Biol. 2018;63:095011.
37. Kase Y, Kanai T, Matsumoto Y, Furusawa Y, Okamoto H, Asaba T, *et al*. Microdosimetric measurements and estimation of human cell survival for heavy-ion beams Radiat Res. 2006;166:629–38.
38. Ballarini F, Altieri S, Bortolussi S, Carante M, Giroletti E, Protti N. The BIANCA model/code of radiation-induced cell death: application to human cells exposed to different radiation types. Radiat Environ Biophys. 2014;53:525–33.
39. Cunha M, Monini C, Testa E, Beuve M. NanOx, a new model to predict cell survival in the context of particle therapy. Phys Med Biol. 2017;62:1248.
40. Sato Y, Furusawa Y. Cell survival fraction estimation based on the probability densities of domain and cell nucleus specific energies using improved microdosimetric kinetic models. Radiat Res. 2012;178(4):341–56.
41. Sato T, Hashimoto S, Inaniwa T, Takada K, Kumada H. Implementation of simplified stochastic microdosimetric kinetic models into PHITS for application to radiation treatment planning. Int J Radiat Biol. 2021;97(10):1450–60.
42. Matsuya Y, Sasaki K, Yoshii Y, Okumura G, Date H. Integrated modelling of cell responses after irradiation for DNA-targeted effects and non-targeted effects. Sci Rep. 2018;8:4849.
43. Matsuya Y, Kai T, Yoshii Y, Yachi Y, Naijo S, Date H, *et al*. Modeling of yield estimation for DNA strand breaks based on Monte Carlo simulations of electron track structure in liquid

water. J Appl Phys. 2019;126:124701.

44. Matsuya Y, Kai T, Sato T, Liamsuwan T, Sasaki K, Nikjoo H. Verification of KURBUC-based ion track structure mode for proton and carbon ions in the PHITS code. Phys Med Biol. 2021;66:06NT02.

45. Matsuya Y, Sato T, Nakamura R, Naijo S, Date H. A theoretical cell-killing model to evaluate oxygen enhancement ratios at DNA damage and cell survival endpoints in radiation therapy. Phys Med Biol. 2020;65:095006.

46. Matsuya Y, McMahon SJ, Tsutsumi K, Sasaki K, Okuyama G, Yoshii Y, *et al*. Investigation of dose-rate effects and cell-cycle distribution under protracted exposure to ionizing radiation for various dose-rates. Sci Rep. 2018;8:8287.

47. Saga R, Matsuya Y, Takahashi R, Hasegawa K, Date H, Hosokawa Y. Analysis of the high-dose-range radioresistance of prostate cancer cells, including cancer stem cells, based on a stochastic model. J Radiat Res. 2019;60(3):298–307.

48. Saga R, Matsuya Y, Sato H, Hasegawa K, Obara H, Komai F, *et al*. Translational study for the clinical outcome of stereotactic body radiotherapy on non-small cell lung cancer based on cell-killing model considering cancer stem-like cells. Radiother Oncol. 2023;181:109444.

49. Matsuya Y, Kai T, Sato T, Ogawa T, Hirata Y, Yoshii Y, *et al*. Track-structure mode in Particle and Heavy Ion Transport code System (PHITS): application to radiobiological research. Int J Radiat Biol. 2022;98:2:148–57.

50. Hirayama H, Namito Y, Bielajew AF, Wilderman SJ, Nelson WR. The EGS5 code system. SLAC Report 730, prepared for the Department of Energy, USA; 2005.

51. Tsuchida H, Kai T, Kitajima K, Matsuya Y, Maejima T, Saito M. Relation between biomolecular dissociation and energy of secondary electrons generated in liquid water by fast heavy ions. Eur Phys J D. 2020;74:212.

52. Incerti S, Kyriakou I, Bordage MC, Guatelli S, Ivanchenko V, Emfietzoglou D. Track structure simulations of proximity functions in liquid water using the Geant4-DNA toolkit. J Appl Phys. 2019;125:104301.

53. Kai T, Yokoya A, Ukai M, Watanabe R. Cross sections, stopping powers, and energy loss rates for rotational and phonon excitation processes in liquid water by electron impact. Radiat Phys Chem. 2015;108:13–7.

54. Kai T, Yokoya A, Ukai M, Fujii K, Watanabe R. Dynamics of low energy electrons in liquid water with consideration of Coulomb interaction with positively charged water molecules induced by electron collision. Radiat Phys Chem. 2014;104:16–22.

55. Kai T, Yokoya A, Ukai M, Watanabe R. Deceleration processes of secondary electrons produced by a high-energy Auger electron in a biological context. Int J Radiat Biol. 2016;92:645–59.

56. Kai T, Yokoya A, Ukai M, Fujii K, Watanabe R. Thermal equilibrium and prehydration processes of electrons injected into liquid water calculated by dynamic Monte Carlo method. Radiat Phys Chem. 2015;115:1–5.

57. Hirata Y, Kai T, Ogawa T, Matsuya Y, Sato T. Implementation of electron track-structure mode for silicon into PHITS for investigating the radiation effects in semiconductor devices. Jpn J Appl Phys. 2022;61:106004.

58. Liamsuwan T, Uehara S, Emfietzoglou D, Nikjoo H. Physical and biophysical properties of proton tracks of energies 1 keV to 300 MeV in water. Int J Radiat Biol. 2011;87:141–60.

59. Liamsuwan T, Nikjoo H. Cross sections for bare and dressed carbon ions in water and neon. Phys Med Biol. 2013;58:641–72.

60. Liamsuwan T, Nikjoo, H. A Monte Carlo track structure simulation code for the full-slowing-down carbon projectiles of energies 1 $keVu^{-1}$–10 $MeVu^{-1}$ in water. Phys Med Biol. 2013;58:673–701.

61. Ogawa T, Hirata Y, Matsuya Y, Kai T. Development of proton track structure model applicable to arbitrary materials. Sci Rep. 2021;11:24401.

62. Kai T, Toigawa T, Matsuya Y, Hirata Y, Tezuka T, Tsuchida H, Yokoya A. Initial yield of hydrated electron production from water radiolysis based on first-principles calculation. RSC Adv. 2023;13:7076–86.

63. Nikjoo H, Goodhead DT, Charlton DE, Paretzke HG. Energy deposition in small cylindrical targets by monoenergetic electrons. Int J Radiat Biol. 1991;60:739–56.

64. Matsuya Y, Nakano T, Kai T, Shikazono N, Akamatsu K, Yoshii Y, *et al*. A simplified cluster analysis of electron track structure for estimating complex DNA damage yields. Int J Mol Sci. 2020;21(5):1701.

65. Matsuya Y, Kai T, Parisi A, Yoshii Y, Sato T. Application of a simple DNA damage model developed for electrons to proton irradiation. Phys. Med. Biol. 2022;67(21):215017.

66. Folkard M, Prise KM, Vojnovic B, Davies S, Roper MJ, Michael BD. Measurement of DNA damage by electrons with energies between 25 and 4000 eV. Int J Radiat Biol. 1993;64:651–58.

67. Botchway SW, Stevens DL, Hill MA, Jenner TJ, O'Neill P. Induction and rejoining of DNA double-strand breaks in Chinese hamster V79-4 cells irradiated with characteristic aluminium K and copper L ultrasoft x-rays. Radiat Res. 1997;148:317–324.

68. de Lara CM, Hill MA, Papworth D, O'Neill P. Dependence of the yield of DNA double-strand breaks in Chinese hamster V79-4 cells on the photon energy of ultrasoft x rays. Radiat Res. 2001;155:440–8.

69. Fulford J, Nikjoo H, Goodhead DT, O'Neill P. Yields of SB and DSB induced in DNA by ALK ultrasoft x-rays and alpha-particles: comparison of experimental and simulated yields. Int J Radiat Biol. 2001;77:1053–66.

70. Leloup C, Garty G, Assaf G, Cristovão A, Breskin A, Chechik R, *et al*. Shchemelinin S, Paz-Elizur T, Livneh Z, Schulte RW, Bashkirov V, Milligan JR, Grosswendt B. Evaluation of lesion clustering in irradiated plasmid DNA. Int J Radiat Biol. 2005;81(1):41–54.

71. Francis Z, Villagrasa C, Clairand I. Simulation of DNA damage clustering after proton irradiation using an adapted DBSCAN algorithm. Comput Methods Programs Biomed. 2011;101(3):265–70.

72. Xu X, Nakano T, Tsuda M, Kanamoto R, Hirayama R, Uzawa A, Ide H. Direct observation of damage clustering in irradiated DNA with atomic force microscopy. Nucleic Acids Res. 2020;48(3):e18.

73. Yachi Y, Matsuya Y, Yoshii Y, Fukunaga H, Date H, Kai T. An analytical method for quantifying complexity of DNA double-strand breaks by γ-H2AX focus formation assay coupled with Monte Carlo track-structure simulation. Int J Mol Sci. 2023;24:1386.

74. Rogakou EP, Boon C, Redon C, Bonner WM. Megabase chromatin domains involved in DNA double-strand breaks in vivo. J Cell Biol. 1999:146:905–16.

75. Sedelnikova OA, Rogakou EP, Panyutin IG, Bonner WM. Quantitative detection of 125IdU-induced DNA double-strand breaks with γ-H2AX antibody. Radiat Res. 2002;158:486–92.

76. Leatherbarrow EL, Harper JV, Cucinotta FA, O'Neill P. Induction and quantification of γ-H2AX foci following low and high LET-irradiation. Int J Radiat Biol. 2006;82:111–8.

77. Nakajima, NI, Brunton H, Watanabe R, Shrikhande A, Hirayama R, Matsufuji N, *et al*. Visualisation of γH2AX foci caused by heavy ion particle traversal; distinction between core track versus non-track damage. PLoS One. 2013;8:e70107.

78. Nikjoo H, O'Neill P, Wilson WE, Goodhead DT. Computational approach for determining the spectrum of DNA damage induced by ionizing radiation. Radiat Res. 2001;156:577–83.

79. Friedland W, Jacob P, Bernhardt P, Paretzke HG, Dingfelder M. Simulation of DNA damage after proton irradiation. Radiat Res. 2003;159:401–10.

80. Matsuya Y, Tsutsumi K, Sasaki K, Date H. Evaluation of the cell survival curve under radiation exposure based on the kinetics of lesions in relation to dose-delivery time. J Radiat Res. 2015;56:90–9.

81. Matsuya Y, Tsutsumi K, Sasaki K, Yoshii Y, Kimura T, Date H. Modeling cell survival and change in amount of DNA during protracted irradiation. J Radiat Res. 2017;58(3):302–12.

82. Matsuya Y, Kimura T, Date H. Markov chain Monte Carlo analysis for the selection of a cell-killing model under high-dose-rate irradiation. Med Phys. 2017;44(10):5522–32.

83. Matsuya Y, McMahon SJ, Ghita M, Yohsii Y, Sato T, Date H, *et al*. Intensity modulated radiation fields induce protective effects and reduce importance of dose-rate effects. Sci Rep. 2019;9:9483.

84. Microdosimetry. Report 36. Rockville: ICRU; 1983.

85. Sato T, Kase Y, Watanabe R, Niita K, Sihver L. Biological dose estimation for charged-particle therapy using an improved PHITS code coupled with a microdosimetric kinetic model. Radiat Res. 2009;171:107–17.

86. Locher GL. Biological effects and therapeutic possibilities of neutrons. Am J Roentgenol. 1936;36:1–13.

87. Coderre JA, Makar MS, Micca PL, Nawrocky MM, Liu HB, Joel DD, *et al*. Amols HI. Derivations of relative biological effectiveness for the high-LET radiations produced during boron neutron capture irradiations of the 9l rat gliosarcoma *in vitro* and *in vivo*. Int J Radiat Oncol. 1993;27:1121–9.

88. Matsuya Y, Ohtsubo Y, Tsutsumi K, Sasaki K, Yamazaki R, Date H. Quantitative estimation of DNA damage by photon irradiation based on the microdosimetric-kinetic model. J Radiat Res. 2014;55:484–93.

89. Park C, Papiez L, Zhang S, Story M, Timmerman RD. Universal survival curve and single fraction equivalent dose: useful tools in understanding potency of ablative radiotherapy. Int J Radiat Oncol Biol Phys. 2008;70:847–52.

90. Astrahan M. Some implications of linear–quadratic–linear radiation dose-response with regard to hypofractionation. Med Phys. 2008;35:4161–72.

91. Brenner DJ. The linear–quadratic model is an appropriate methodology for determining isoeffective doses at large doses per fraction. Semin Radiat Oncol. 2008;18:234–39.

92. Lyng FM, Maguire P, McClean B, Seymour C, Mothersill C. The involvement of calcium and MAP kinase signaling pathways in the production of radiation-induced bystander effects. Radiat Res. 2006;165(4):400–9.

93. Matsumoto H, Hayashi S, Hatashita M, Ohnishi K, Shioura H, Ohtsubo T, *et al*. Induction of radioresistance by a nitric oxide-mediated bystander effect. Radiat Res. 2001;155:387–96.

94. Stewart RD, Ratnayake RK, Jennings K. Microdosimetric model for the induction of cell killing through medium-bone signals. Radiat Res. 2006;165:460–9.

95. Liu ZF, Prestwich WV, Stewart RD, Byun SH, Mothersill CE, McNeill FE, *et al*. Effective target size for the induction of bystander effects in medium transfer experiments. Radiat Res. 2007;168:627–30.

96. Hei TK, Zhou H, Ivanov VN, Hong M, Lieberman HB, Brenner DJ, *et al*. Mechanism of radiation-induced bystander effects: a unifying model. J Pharm Pharmacol. 2008;60(8):943–50.

97. Saga R, Matsuya Y, Takahashi R, Hasegawa K, Date H, Hosokawa Y. 4-Methylumbelliferone administration enhances radiosensitivity of human fibrosarcoma by intercellular communication. Sci Rep. 2021;11:8258.

98. Matsuya Y, McMahon SJ, Butterworth KT, Naijo S, Nara S, Yachi Y, *et al*. Oxygen enhancement ratios of cancer cells after exposure to intensity modulated x-ray fields: DNA damage and cell survival. Phys Med Biol. 2023;66:075014.

99. Matsuya Y, McMahon SJ, Butterworth KT, Yachi Y, Saga R, Sato T, *et al*. Modelling oxygen effects on the in- and out-of-field radiosensitivity of cells exposed to intensity-modulated radiation fields. Phys Med Biol. 2023;68:095008.

100. Bao B, Ahmad A, Azmi AS, Ali S, Sarkar FH. Overview of cancer stem cells (CSCs) and mechanisms of their regulation: implications for cancer therapy. Curr Protoc Pharmacol. 2013;61:14.25.1–14.25.14.

101. Withers HR. The four R's of radiotherapy. Adv Radiat Biol. 1975;5:241–71.

102. Steel GG, McMillan TJ, Peacock JH. The 5Rs of radiobiology. *Int J Radiat Biol*. 1989;56:1045–8.

103. Alfonso JCL, Berk L. Modeling the effect of intratumoral heterogeneity of radiosensitivity on tumor response over the course of fractionated radiation therapy. Radiat Oncol. 2019;14:88.

104. Fukui R, Saga R, Matsuya Y, Tomita K, Kuwahara Y, Ohuchi K, *et al*. Tumor radioresistance caused by radiation-induced changes of stem-like cell content and sub-lethal damage repair capability. Sci Rep. 2022;12:1056.

105. Kuwahara Y, Mori M, Oikawa T, Shimura T, Ohtake Y, Mori S, *et al*. The modified high-density survival assay is the useful tool to predict the effectiveness of fractionated radiation exposure. J Radiat Res. 2010;51(3):297–302.

106. Aoki M, Hatayama Y, Kawaguchi H, Hirose K, Sato M, Akimoto H, *et al*. Clinical outcome of stereotactic body radiotherapy for primary and oligometastatic lung tumors: a single institutional study with almost uniform dose with different five treatment schedules. Radiat Oncol. 2016;11:5.

107. Sato H, Ito F, Hasegawa K, Saga R, Hosokawa Y, Tanaka M, *et al*. Identification of novel prognostic factors focusing on clinical outcomes in patients with non-small cell lung cancer after stereotactic body radiotherapy. Oncol Lett. 2022;23:79.

108. Sato T, Matsuya Y, Hamada N. Microdosimetric modeling of relative biological effectiveness for skin reactions: possible linkage between in vitro and in vivo data. Int J Radiat Oncol Biol Phys. 2022;114(1):153–62.